Int. J. Electrochem. Sci., 16 **(2021)** Article ID: 210411, doi: 10.20964/2021.04.27

International Journal of
ELECTROCHEMICAL
SCIENCE
www.electrochemsci.org

Electrochemical sensor based on molecularly imprinted film for high sensitivity detection of clenbuterol prepared using sol-gel method

Li Liu[1], *Chenghong Long*[1], *Shenghui Wei*[2,*], *Yu Sun*[3]

[1] Sports Department, Chongqing Jiaotong University, Chongqing, 400074, China
[2] College of Physical and Health Science, Chongqing Normal University, Chongqing, 401331, China
[3] Basic Science Department, Wuchang Shouyi University, Wuhan Hubei, 430064, China
[*]E-mail: weishenghui@vtcuni.com

Received: 15 December 2020 / *Accepted:* 24 January 2021 / *Published:* 28 February 2021

The determination of clenbuterol is crucial for food safety and sport science. In this work, we use tetraethyl orthosilicate and (3-aminopropyl)triethoxysilane as cross-linking agents and functional monomers for the electrodeposition of SiO_2 films with the addition of clenbuterol. After the elution process, the prepared electrode can be used for the sensitive determination of clenbuterol due to the molecular imprinting effect. Under optimum conditions, results show that the current of clenbuterol decreases linearly in the range of 2 μM to 0.1 mM, and the detection limit is 31 nM. The proposed electrochemical sensor also exhibits excellent stability and reproducibility, showing its high potential for use in sensing clenbuterol in food samples.

Keywords: Clenbuterol; Sol-gel; SiO_2; Electrodeposition; Molecular imprinting

1. INTRODUCTION

β-agonists are phenylethanolamine compounds in veterinary drug residues. At present, clenbuterol, salbutamol and terbutaline are the most common veterinary drugs. These β-agonists can enhance lipolysis and slow protein catabolism, promote muscle tissue growth and reduce carcass tissue content [1,2]. Therefore, they are used in large doses in animal husbandry production, which can significantly improve the feed conversion rate and lean meat rate; furthermore, these β-agonists are often used as growth-promoting additives in new drugs. β-agonists have a chemical structure similar to adrenaline and can bind with receptors on the cell surface to produce obvious physiological effects, such as palpitations, headaches, dizziness, nausea, vomiting, fevers, muscle tremors, nervousness, blood expansion, and accelerated heart rates. Moreover, due to the oral activity of these compounds, β-agonist residues will concentrate in edible animal tissues [3–5]. If you eat too much, it will produce certain toxic

side effects on human and animal livers, kidneys and other internal organs. Moreover, if athletes eat these β-agonists by mistake in their daily diet, it may lead to being banned by testing positive in doping tests [6]. β-agonist residues in animal-derived food seriously hinder the export trade of animal-derived food and threaten the safety of people's lives. Therefore, we should strengthen the detection and control of β-agonist veterinary drug residues in animal feed and food [7–9].

At present, the detection methods of β-agonist veterinary drugs are mainly divided into two categories: chromatographic analysis technology and immunoassay technology. High-performance liquid chromatography (HPLC) [10–12], gas chromatography-mass spectrometry (GC-MS) [13–15] and capillary zone electrophoresis (CE) [16–18] are the most commonly used techniques for the detection of veterinary drug residues. HPLC has the characteristics of a low detection limit, simple operation, fast response, good reproducibility, and accurate and reliable results. GC-MS can be used for the qualitative and quantitative analysis of certain residues in the presence of multiple residues. Therefore, GC-MS can effectively detect various veterinary drug residues in food. However, these two methods also have the characteristics of a cumbersome detection process, long detection time, expensive instruments, difficult operation and high price. Alternatively, the electrochemical sensing method can be considered a new technique for the sensing of β-agonists due to its high sensitivity and fast response. Molecularly imprinted electrochemical sensors can be used for the quantitative detection of target molecules or analogues by specific selective recognition [19–22]. These sensors have good stability and can be used in harsh environments, including those consisting of high temperatures, high pressures, organic solvents, acids, alkali, etc.

Sol-gel technology is a promising material processing method. It has been widely applied in material science and many related fields. This technology refers to the way that organic or inorganic compounds are solidified by solution, sol and gel, and then heat treated to produce oxides or other compounds [23–30]. Especially in the past 20 years, sol-gel technology has shown wide application prospects in regard to producing thin films, ultrafine powders, composite functional materials, fibres and glass with high melting points [31,32]. The application value of the sol-gel process is that it has the advantages of high purity, strong uniformity, low treatment temperature and easy control of reaction conditions. Compared with other materials, sol-gel materials have better physical rigidity and chemical inertia, negligible swelling in solvents, and high stability to light, chemicals, heat and biodegradation.

At present, the molecularly imprinted film formed by a silica sol-gel is nano- to microscale and porous. The material diffusion rate in the film is relatively fast, and the preparation method is simple. The formed film has the advantages of physical rigidity and chemical and thermal stability [33–36]. The sol-gel films prepared on the electrode surface are mostly made by drop coating, spin coating or physical adsorption. Although this method is fast and simple, it is difficult to control the thickness of molecularly imprinted films and avoid cracking caused by surface tension. Therefore, in the process of electrodeposition, silanes are hydrolysed, condensed and dealcoholized to form a dense silica-like network structure. Compared with a traditional silica gel molecularly imprinted film prepared by the traditional method, the gelatinization process and evaporation process are separated from each other in the above preparation process so that silane is fully hydrolysed and dried and is more conducive to the diffusion of substances in the film; this method effectively avoids film cracking. In this work, we

fabricate a SiO_2-clenbuterol molecularly imprinted electrochemical sensor. The sensor has the advantages of high stability, a long service life and fast response.

2. MATERIALS AND METHOD

All reagents were analytical grade and used without purification. Tetraethyl orthosilicate (TEOS), 3-aminopropyl)triethoxysilane (APTES), and clenbuterol were purchased from Aladdin Co., Ltd. A gold electrode (Au), Pt wires and Ag/AgCl (3 M) were used as the working, counter and reference electrodes, respectively. The morphology was observed by scanning electron microscopy (SEM, Apreo, FEI). The surface functional groups were characterized by Fourier transform infrared (FTIR) spectroscopy (Nicolet iS5, Thermo Scientific).

The Au was first polished using an Al_2O_3 slurry and washed with water and ethanol. Then, the Au was added to the electrodeposited sol-gel solution. The sol-gel solution was prepared with 0.5 mL of TEOS, 0.2 mL of APTES, 0.02 g of clenbuterol, and 4 mL of KCl (0.4 M) with 2 mL of ethanol. The deposition process (molecular imprinting) was conducted at -0.8 V for 30 min. The electrodeposited Au was then washed using water and naturally dried. The prepared sensor was denoted as Cl/MIP/Au. The electrochemical sensor without the target molecule was prepared using a similar method without adding clenbuterol and denoted as MIP/Au. During sensing, the prepared Cl/MIP/Au was first immersed in 50% HNO_3 for half an hour to remove clenbuterol molecules (elution process). Then, Cl/MIP/Au was used for the detection of different concentrations of clenbuterol using potassium ferricyanide as a probe.

3. RESULTS AND DISCUSSION

SEM was used to characterize the surface morphology of the film. Fig. 1a is the SEM image of the molecularly imprinted film before elution. It can be seen from the figure that the surface of the film is smooth before the template molecules are eluted. Fig. 1b is the SEM image of the molecularly imprinted film after elution. It can be seen from the figure that dense molecularly imprinted holes appear on the surface of the film after the elution of template molecules, and the surface becomes rough. These results show that the SiO_2 molecularly imprinted film can imprint clenbuterol with high stability.

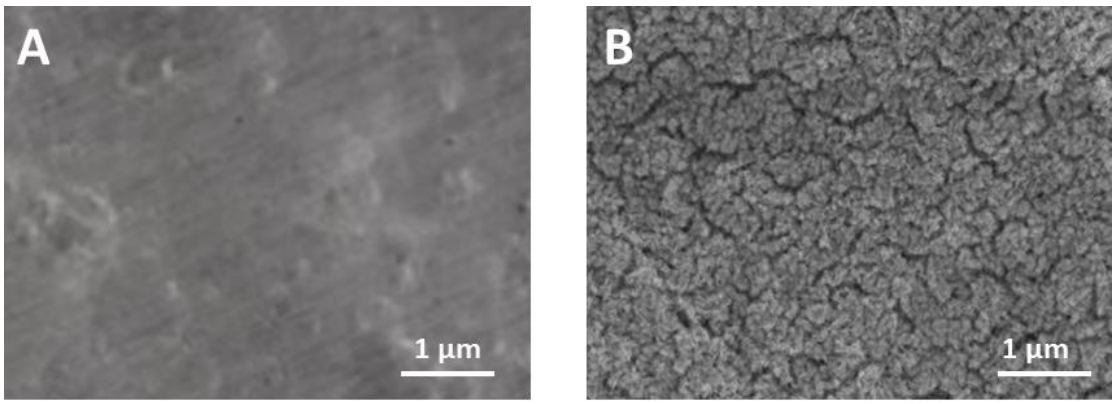

Figure 1. SEM image of Cl/MIP/Au (A) before and (B) after the elution process.

The structure and composition of the molecularly imprinted film were studied by FTIR spectroscopy. As shown in Fig. 2, both the molecularly imprinted polymer and nonmolecularly imprinted polymer have a stretching vibration peak of -N-H at 3425 cm^{-1}. Additionally, they all have a strong absorption peak of -Si-O at 1083 cm^{-1}, which indicates that the main component of the molecularly imprinted film and nonmolecularly imprinted film is SiO_2. The molecular imprinted polymer shows a skeleton vibration peak of -C_6-H_6 at 1590 cm^{-1} and a fingerprint absorption peak of -C_6-H_6 at 693-868 cm^{-1}. These results show that the target molecule clenbuterol is successfully imprinted in the SiO_2 film [37–39].

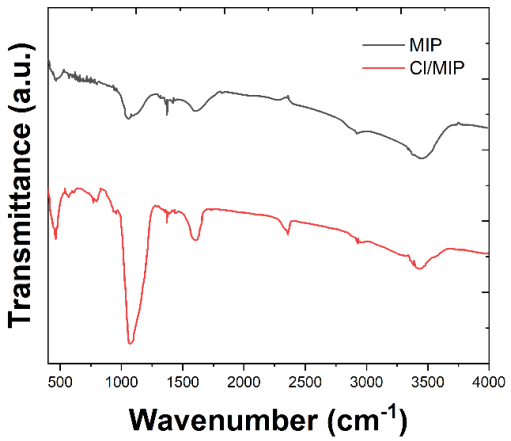

Figure 2. FTIR of Cl/MIP and MIP/Au.

The polymerization conditions of the molecularly imprinted film were optimized. We set the amount of template molecules, changed the mass ratio of the functional monomer to crosslinker, and finally determined the differential pulse voltammetry (DPV) peak height of each sensor after elution under the same conditions. As shown in Fig. 3, after repeated tests on the ratio of the template molecule, functional monomer and crosslinking agent, it is found that the optimum ratio of the crosslinker, functional monomer and template molecule is 25:10:1, respectively.

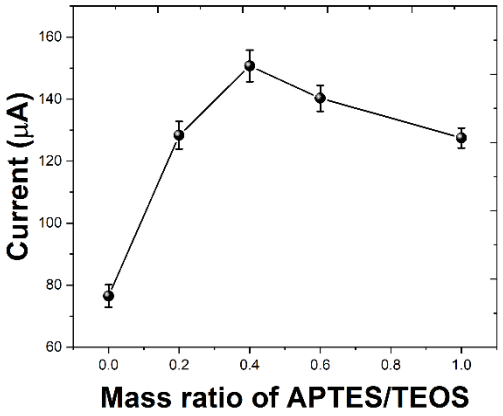

Figure 3. DPV peak current of different ratios of APETS/TEOS (0.1 M PBS, pH 7.0, at a scan rate of 10 mV/s).

Cyclic voltammetry (CV) and electrochemical impedance spectroscopy (EIS) were used to characterize the properties of the films. Since clenbuterol has no electrochemical activity, the molecularly imprinted membrane was characterized by an indirect method. We used potassium hexacyanoferrate as the probe between the imprinted electrode and the bottom solution, and the electrochemical signal changed accordingly when holes in the membrane were blocked. The imprinted holes in the membrane provide a mass transfer channel for the redox reaction between the probe molecules and electrode surface. After the imprinted hole readsorbs the template molecule, the hole is blocked, which hinders the process of potassium ferricyanide probe molecules entering the hole and contacting the electrode surface; therefore, the decreased amount of potassium ferricyanide reaching the electrode surface changes the current value accordingly. These current values reflect the change in the molecular weight of the template in solution. As shown in Fig. 4, curves a to b show the process of obtaining a molecularly imprinted polymer film on a bare gold electrode. The formation of a nonconductive molecularly imprinted film on the electrode surface hinders the redox reaction process of potassium ferricyanide probe molecules arriving at the electrode surface. The redox peak current of potassium ferricyanide decreases sharply from the bare gold electrode to Cl/MIP/Au. Curves b to c are the elution process of template molecules. Because the template molecules are eluted and the imprinted holes are exposed, the potassium ferricyanide probe molecules can contact the electrode surface through the imprinted holes and undergo a redox reaction, which makes the peak current value of potassium ferricyanide sharply increase from curve b (after modifying the molecularly imprinted membrane) to curve c (after eluting the template molecules). Curves c to d are the process of readsorption of template molecules. When the template molecules re-enter the imprinted hole, the redox of potassium ferricyanide probe molecules on the electrode surface becomes more difficult, so the peak current value sharply decreases. These changes indicate that the molecularly imprinted membrane is specific and efficient for the recognition of clenbuterol [40–43].

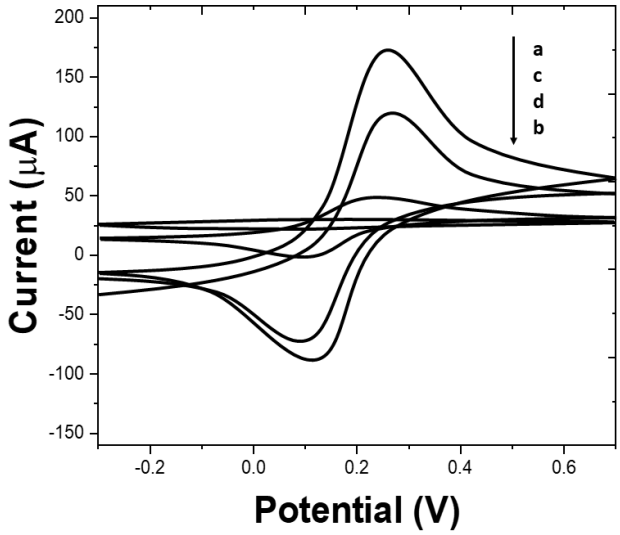

Figure 4. CVs (5 mM $K_3[Fe(CN)_6]/K_4[Fe(CN)_6$, at a scan rate of 50 mV/s) of bare Au (a), Cl/MIP/Au before elution (b), Cl/MIP/Au after elution (c) and adding clenbuterol into Cl/MIP/Au (d).

Figure 5 shows the CV curves of Au and MIP/Au. The formation of a polymer film on the electrode surface makes the redox reaction between the electrode surface and the bottom solution more difficult, which makes the current value of potassium ferricyanide sharply decrease from that with just Au. In the subsequent elution process, due to the lack of template molecules, molecularly imprinted holes will no longer appear on the polymer film, so the current will hardly increase.

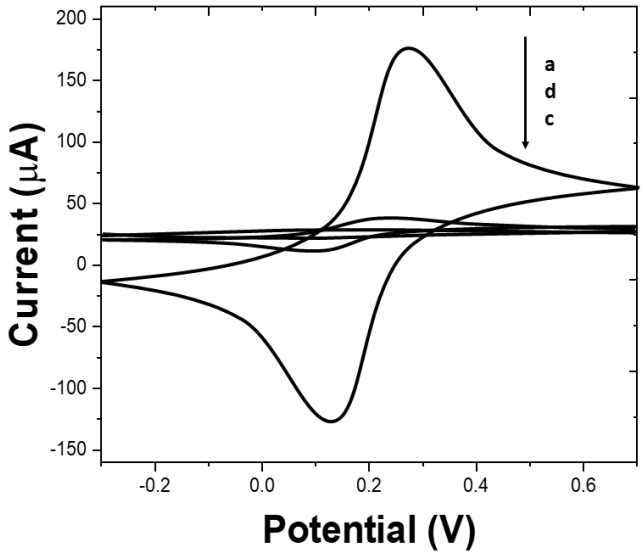

Figure 5. CVs (5 mM $K_3[Fe(CN)_6]/K_4[Fe(CN)_6$, at a scan rate of 50 mV/s) of bare Au (a) and MIP/Au.

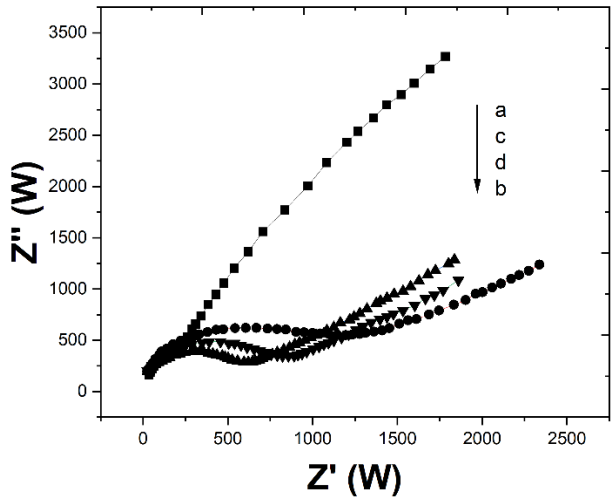

Figure 6. EIS (5 mM $K_3[Fe(CN)_6]/K_4[Fe(CN)_6]$) of bare Au (a), Cl/MIP/Au before elution (b), Cl/MIP/Au after elution (c) and adding clenbuterol into Cl/MIP/Au (d).

Figure 6 shows the EIS spectra. During the formation of a molecularly imprinted film, the electron mass transfer between the bottom solution and electrode surface becomes more difficult due to the formation of a molecularly imprinted film on the electrode surface. Therefore, after each step of assembly, we can see an increase in impedance. However, after the elution process, the impedance of

the electrode recovers somewhat [44–47] due to the disappearance of clenbuterol on the electrode surface.

Therefore, the resistance of the electrode increases and the conductivity decreases. During the process of elution, almost all template molecules are removed, so the potassium ferricyanide probe molecules can reach the electrode surface through the molecularly imprinted holes and undergo a redox reaction; this mechanism leads to another increase in conductivity [48–51]. After the imprinted molecules are adsorbed again, the mass transfer channel of the potassium ferricyanide probe molecule is again blocked; thus, the resistance increases again, and the conductivity sharply decreases. The above changes also indicate that the molecularly imprinted film is specific and efficient for the recognition of the template molecule clenbuterol. The advantage of this approach is that expensive biological reagents can be avoided.

DPV can be used to detect the response of clenbuterol in imprinted films. As shown in Fig. 7, with the addition of 2 μM clenbuterol to a 10 mL PBS solution with potassium ferricyanide, the oxidation peak current of potassium ferricyanide gradually decreases. In the range of 2 μM to 0.1 mM, the peak current of potassium ferricyanide decreases linearly with an increasing clenbuterol concentration. The linear equation is I=-0.829 + 0. 9711c (r = 0. 9979). According to S/N=3, the detection limit of clenbuterol is 31 nM. Compared with other sensors listed in Table 1 for the detection of clenbuterol, the detection performance of Cl/MIP/Au in this work is superior to that of the majority of materials in the previous reports.

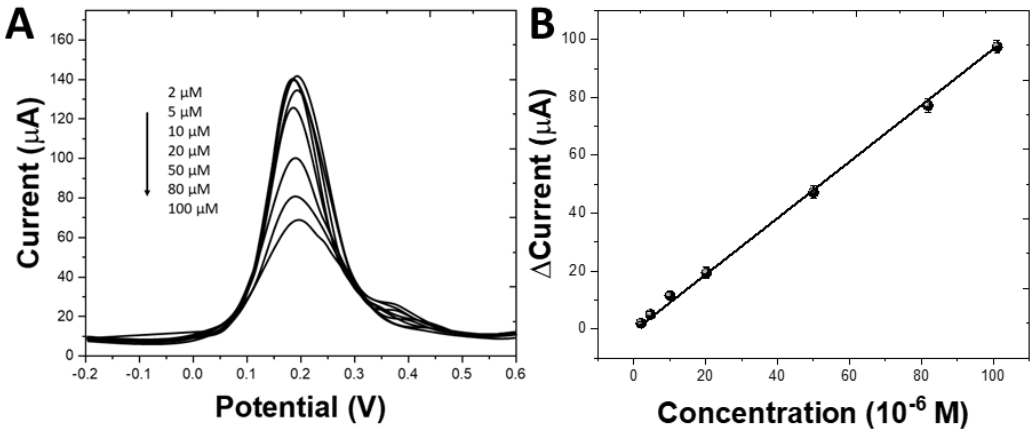

Figure 7. (A) DPV (0.1 M PBS, pH 7.0, at a scan rate of 10 mV/s) responses of Cl/MIP/Au towards clenbuterol from 2 μM to 0.1 mM. (B) Calibration curve for electrochemical response.

The reproducibility of the response was achieved by measuring the response current of 0.05 mM clenbuterol with the same imprinted electrode, and the results are -130.7 μA, -137.9 μA, -131.3 μA, -139.1 μA and -133.4 μA, respectively. The relative standard deviation is 4.1%, indicating that the imprinted electrode has good reproducibility. To ensure the reproducibility of the electrode, the electrode was immersed in a 1:1 nitric acid/ethanol system for 10 min after each measurement. The results show that there is reversible binding between clenbuterol and the recognition sites in the imprinted membrane.

The background response can be completely recovered, suggesting excellent reversibility and reproducibility.

Table 1. The detection performance of clenbuterol by various electrochemical sensor.

Sensor	Detection limit (μM)	Linear range (μM)	Ref
Nafion–Au/GCE	0.1	0.8-10	[52]
MoS_2-Au-PEI-hemin	1.92	10–2000	[53]
Poly(3,4-ethylenedioxythiophene)/graphene oxide	0.15	1-40	[54]
BDD	0.066	0.1-100	[55]
Cl/MIP/Au	0.031	2- 100	This work

In addition, the current response of the sensor can reach equilibrium after 120 s in 0.05 mM clenbuterol. Compared with a conventional polymer film electrochemical sensor, the equilibrium time of Cl/MIP/Au is reduced, and the sensor response is faster.

The validation of the developed clenbuterol electrochemical sensor in real samples was investigated using spiked milk. The sensing performance results were compared with ELISA tests (Table 2), and the standard addition method was applied. The recovery of Cl/MIP/Au is in the range of 97.90 to 103.57%, suggesting good reliability.

Table 2. Real sample analysis using Cl/MIP/Au and ELISA test.

		Cl/MIP/Au			**ELISA**		
Sample	**Added**	**Detected**	**Recovery**	**RSD**	**Detected**	**Recovery**	**RSD**
Milk 1	10.00 μM	9.79 μM	97.90%	3.3%	10.17 μM	101.70%	4.1%
Milk 2	30.00 μM	31.07μM	103.57%	2.7%	32.06 μM	106.87%	5.2%

4. CONCLUSIONS

A nanosized silica molecularly imprinted film of clenbuterol was synthesized on the surface of Au by electrochemical deposition using APTES as the functional monomer and TEOS as the cross-linking agent. The molecularly imprinted film could be used as an electrochemical sensor of clenbuterol by using potassium ferricyanide as an ion probe. The results showed that the current of clenbuterol decreased linearly in the range of 2 μM to 0.1 mM, and the detection limit was 31 nM. The experimental results show that the SiO_2 molecularly imprinted film formed by the simple electrochemical sol-gel

deposition is porous and the film has a high molecular diffusion rate. Furthermore, the formed film has the advantages of physical rigidity and chemical and thermal stability.

References

1. Y. Ge, M.B. Camarada, L. Xu, M. Qu, H. Liang, E. Zhao, M. Li, Y. Wen, *Microchim. Acta*, 185 (2018) 566.
2. J. Liu, Y. Qin, H. Zhu, J. Zhao, *Chin. J. Anal. Chem.*, 46 (2018) 225–231.
3. X. Lin, Y. Ni, X. Pei, S. Kokot, *Anal. Methods*, 9 (2017) 1105–1111.
4. Y. Ge, M. Qu, L. Xu, X. Wang, J. Xin, X. Liao, M. Li, M. Li, Y. Wen, *Microchim. Acta*, 186 (2019) 836.
5. X. Xiao, Y. Wang, W. Tan, H. Liu, Y. Duan, X. Zhang, D. Zhang, Y. Jiang, J. Wang, J. Gong, J. Ma, T. Yang, Z. Tong, *Electroanalysis*, 30 (2018) 2744–2749.
6. Y. Tang, J. Gao, X. Liu, X. Gao, T. Ma, X. Lu, J. Li, *Food Chem.*, 228 (2017) 62–69.
7. X. Jin, G. Fang, M. Pan, Y. Yang, X. Bai, S. Wang, *Biosens. Bioelectron.*, 102 (2018) 357–364.
8. T. Simon, M. Shellaiah, P. Steffi, K.W. Sun, F.-H. Ko, *Anal. Chim. Acta*, 1023 (2018) 96–104.
9. Q. Huang, T. Bu, W. Zhang, L. Yan, M. Zhang, Q. Yang, L. Huang, B. Yang, N. Hu, Y. Suo, J. Wang, D. Zhang, *Food Chem.*, 262 (2018) 48–55.
10. L. Ma, A. Nilghaz, J.R. Choi, X. Liu, X. Lu, *Food Chem.*, 246 (2018) 437–441.
11. M. Li, Y. Zhang, Y. Xue, X. Hong, Y. Cui, Z. Liu, D. Du, *Food Control*, 73 (2017) 1039–1044.
12. Y. Tang, J. Gao, X. Liu, X. Gao, T. Ma, X. Lu, J. Li, *Food Chem.*, 228 (2017) 62–69.
13. F. Feng, J. Zheng, P. Qin, T. Han, D. Zhao, *Talanta*, 167 (2017) 94–102.
14. J. Cheng, S. Wang, S. Zhang, P. Wang, J. Xie, C. Han, X.-O. Su, *Sens. Actuators B Chem.*, 279 (2019) 7–14.
15. P. Guo, Z. Luo, X. Xu, Y. Zhou, B. Zhang, R. Chang, W. Du, C. Chang, Q. Fu, *Food Chem.*, 217 (2017) 628–636.
16. X. Hu, H. Zhang, S. Chen, R. Yuan, J. You, *Anal. Bioanal. Chem.*, 410 (2018) 7881–7890.
17. P.K. Kalambate, S.S. Upadhyay, Y. Shen, W. Laiwattanapaisal, Y. Huang, *J. Materiomics*, 7 (2021) 226–235.
18. G. Yang, C. Zhu, X.-H. Liu, Y. Wang, F. Qu, *Chin. J. Anal. Chem.*, 46 (2018) 1595–1603.
19. X. Zhu, Y. Zeng, Z. Zhang, Y. Yang, Y. Zhai, H. Wang, L. Liu, J. Hu, L. Li, *Biosens. Bioelectron.*, 108 (2018) 38–45.
20. Z. Mazouz, M. Mokni, N. Fourati, C. Zerrouki, F. Barbault, M. Seydou, R. Kalfat, N. Yaakoubi, A. Omezzine, A. Bouslema, A. Othmane, *Biosens. Bioelectron.*, 151 (2020) 111978.
21. S. Rebocho, C.M. Cordas, R. Viveiros, T. Casimiro, *J. Supercrit. Fluids*, 135 (2018) 98–104.
22. Y. Ma, C. Liu, M. Wang, L.-S. Wang, *Talanta*, 196 (2019) 486–492.
23. B. Deiminiat, G.H. Rounaghi, M.H. Arbab-Zavar, *Sens. Actuators B Chem.*, 238 (2017) 651–659.
24. A. Salehabadi, F. Sarrami, M. Salavati-Niasari, T. Gholami, D. Spagnoli, A. Karton, *J. Alloys Compd.*, 744 (2018) 574–582.
25. Y. Zhang, P. Xin, Q. Yao, *J. Alloys Compd.*, 741 (2018) 404–408.
26. L. Fu, Y. Zheng, P. Zhang, H. Zhang, M. Wu, H. Zhang, A. Wang, W. Su, F. Chen, J. Yu, W. Cai, C.-T. Lin, *Bioelectrochemistry*, 129 (2019) 199–205.
27. L. Fu, Y. Zheng, P. Zhang, H. Zhang, Y. Xu, J. Zhou, H. Zhang, H. Karimi-Maleh, G. Lai, S. Zhao, W. Su, J. Yu, C.-T. Lin, *Biosens. Bioelectron.*, 159 (2020) 112212.
28. L. Fu, A. Wang, K. Xie, J. Zhu, F. Chen, H. Wang, H. Zhang, W. Su, Z. Wang, C. Zhou, S. Ruan, *Sens. Actuators B Chem.*, 304 (2020) 127390.
29. Y. Xu, Y. Lu, P. Zhang, Y. Wang, Y. Zheng, L. Fu, H. Zhang, C.-T. Lin, A. Yu, *Bioelectrochemistry*, 133 (2020) 107455.
30. L. Fu, M. Wu, Y. Zheng, P. Zhang, C. Ye, H. Zhang, K. Wang, W. Su, F. Chen, J. Yu, A. Yu, W. Cai,

C.-T. Lin, *Sens. Actuators B Chem.*, 298 (2019) 126836.
31. H. Ashassi-Sorkhabi, S. Moradi-Alavian, M.D. Esrafili, A. Kazempour, *Prog. Org. Coat.*, 131 (2019) 191–202.
32. A. Anancia Grace, K.P. Divya, V. Dharuman, J.H. Hahn, *Electrochimica Acta*, 302 (2019) 291–300.
33. L. Saleh Ghadimi, N. Arsalani, I. Ahadzadeh, A. Hajalilou, E. Abouzari-Lotf, *Appl. Surf. Sci.*, 494 (2019) 440–451.
34. X. Zou, F. Shang, S. Wang, *Spectrochim. Acta. A. Mol. Biomol. Spectrosc.*, 173 (2017) 843–848.
35. S. Maitra, P.K. Chakraborty, R. Mitra, T.K. Nath, *Curr. Appl. Phys.*, 20 (2020) 1404–1415.
36. A. Cassel, B. Fleutot, M. Courty, V. Viallet, M. Morcrette, *Solid State Ion.*, 309 (2017) 63–70.
37. F.V. Grigoriev, V.B. Sulimov, A.V. Tikhonravov, *J. Non-Cryst. Solids*, 512 (2019) 98–102.
38. F.H. Rajab, Z. Liu, L. Li, *Appl. Surf. Sci.*, 427 (2018) 1135–1145.
39. J. Guo, D. Benz, T.-T. Doan Nguyen, P.-H. Nguyen, T.-L. Thi Le, H.-H. Nguyen, D. La Zara, B. Liang, H.T. (Bert) Hintzen, J.R. van Ommen, H. Van Bui, *Appl. Surf. Sci.*, 530 (2020) 147244.
40. A. Motaharian, M.R.M. Hosseini, K. Naseri, *Sens. Actuators B Chem.*, 288 (2019) 356–362.
41. P. Luliński, *Mater. Sci. Eng. C*, 76 (2017) 1344–1353.
42. R. Khosrokhavar, A. Motaharian, M.R. Milani Hosseini, S. Mohammadsadegh, *Microchem. J.*, 159 (2020) 105348.
43. R.J. Weaver, C. Betts, E.A. Blomme, H.H. Gerets, K. Gjervig Jensen, P.G. Hewitt, S. Juhila, G. Labbe, M.J. Liguori, N. Mesens, *Expert Opin. Drug Metab. Toxicol.*, 13 (2017) 767–782.
44. H. Karimi-Maleh, Y. Orooji, A. Ayati, S. Qanbari, B. Tanhaei, F. Karimi, M. Alizadeh, J. Rouhi, L. Fu, M. Sillanpää, *J. Mol. Liq.* (2020) 115062.
45. H. Karimi-Maleh, B.G. Kumar, S. Rajendran, J. Qin, S. Vadivel, D. Durgalakshmi, F. Gracia, M. Soto-Moscoso, Y. Orooji, F. Karimi, *J. Mol. Liq.*, 314 (2020) 113588.
46. L. Fu, Z. Liu, J. Ge, M. Guo, H. Zhang, F. Chen, W. Su, A. Yu, *J. Electroanal. Chem.*, 841 (2019) 142–147.
47. J. Zhou, Y. Zheng, J. Zhang, H. Karimi-Maleh, Y. Xu, Q. Zhou, L. Fu, W. Wu, *Anal. Lett.*, 53 (2020) 2517–2528.
48. Z. Shamsadin-Azad, M.A. Taher, S. Cheraghi, H. Karimi-Maleh, *J. Food Meas. Charact.*, 13 (2019) 1781–1787.
49. H. Karimi-Maleh, F. Karimi, Y. Orooji, G. Mansouri, A. Razmjou, A. Aygun, F. Sen, *Sci. Rep.*, 10 (2020) 11699.
50. H. Karimi-Maleh, F. Karimi, S. Malekmohammadi, N. Zakariae, R. Esmaeili, S. Rostamnia, M.L. Yola, N. Atar, S. Movaghgharnezhad, S. Rajendran, A. Razmjou, Y. Orooji, S. Agarwal, V.K. Gupta, *J. Mol. Liq.*, 310 (2020) 113185.
51. H. Karimi-Maleh, F. Karimi, M. Alizadeh, A.L. Sanati, *Chem. Rec.*, 20 (2020) 682–692.
52. L. Liu, H. Pan, M. Du, W. Xie, J. Wang, *Electrochimica Acta*, 55 (2010) 7240–7245.
53. Y. Yang, H. Zhang, C. Huang, D. Yang, N. Jia, *Biosens. Bioelectron.*, 89 (2017) 461–467.
54. N.A.A. Talib, F. Salam, Y. Sulaiman, *Sensors*, 18 (2018) 4324.
55. Z. Ma, Q. Wang, N. Gao, H. Li, *Microchem. J.*, 157 (2020) 104911.